Early Detection of Central Visual Function Decline in Cone–Rod Dystrophy by the Use of Macular Focal Cone Electroretinogram

Lucia Galli-Resta,[1] Marco Piccardi,[2] Lucia Ziccardi,[3] Antonello Fadda,[4] Angelo Minnella,[2] Dario Marangoni,[2] Giorgio Placidi,[2] Giovanni Resta,[5] and Benedetto Falsini[2]

[1]Istituto di Neuroscienze Consiglio Nazionale delle Ricerche (CNR), Pisa, Italy
[2]Institute of Ophthalmology, Policlinico Gemelli, Catholic University, Rome, Italy
[3]Bietti Foundation, Istituto di Ricovero e Cura a Carattere Scientifico (IRCCS), Rome, Italy
[4]Tecnologie e Salute, Istituto Superiore di Sanità, Rome, Italy
[5]Istituto di Informatica e Telematica CNR, Pisa, Italy

PURPOSE. To evaluate macular focal cone ERG (fERG) as a tool for reliable and early detection of central retinal function decay in cone-rod dystrophy (CRD).

METHODS. A retrospective study of the time course of fERG amplitude and its relation to visual acuity alterations was performed in 47 CRD patients followed yearly for 6.0 ± 3.1 years. Macular focal cone ERG was evoked by a flickering uniform red field overlaying the central 18° of visual field.

RESULTS. Macular focal cone ERG follow-up allowed a clear-cut identification of CRD patients as stationary or progressive, in agreement with visual acuity follow-up. In all progressive patients, fERG declined whenever visual acuity declined, and—in 50% of the cases—fERG loss anticipated acuity loss of several years.

CONCLUSIONS. Macular focal cone ERG represents a sensitive assay to detect, categorize, and follow the progression of central retinal dysfunction in CRD. Its use as a diagnostic tool in CRD may help anticipate, for an individual patient, the likelihood and rate of further disease progression before visual acuity loss has occurred.

Keywords: cone-rod dystrophy, focal ERG, visual acuity

Cone-rod dystrophies (CRDs) are a group of inherited retinal disorders representing a major cause of blindness in children and young adults.[1,2] Cone-rod dystrophies are characterized by early decline of visual acuity and loss of sensitivity in the central visual field, photosensitivity, and color vision deficits, later followed by progressive loss in peripheral vision.[1,3] During the course of the disease, pigmentary changes of the macula and a midperipheral pigmentation become apparent. Full-field ERG shows abnormalities of both cone and rod responses, with cone responses typically more severely and more precociously affected than rod responses.[3–8]

The natural history of CRDs is known to be variable, reflecting the clinical and genetic heterogeneity of this group of diseases. The disease can be stationary or progressive, with variable age of visual decay onset. Landmark studies employed ERG, dark-adaptometry visual acuity loss, fundus imaging, and modified perimetric techniques to describe the different subtypes of functional CRD phenotypes.[3–8,9] These phenotypes are now being matched with the emerging molecular genetic classification of the disease.[2,5,10–13]

Yet, at present, few clinical studies have longitudinally evaluated the rate of retinal function loss in progressive CRD forms,[5,12,14] and reliable diagnostic tools for an early identification of the patient risk of decay are still under investigation.[10,15] To contribute to this effort, we present here a retrospective longitudinal study testing the clinical effectiveness of the macular focal cone ERG (fERG) recorded over the central 18° of visual field for monitoring, phenotyping, and anticipating CRD progression in the central retina.

METHODS

Patients

This is a retrospective study based on the database of CRD patients clinically followed at the Visual Electrophysiology Service of the Institute of Ophthalmology at the Università Cattolica del Sacro Cuore in Rome, Italy. Patients had sought consultation because of visual symptoms. Following the first visit, they were invited to adhere to the Institutional schedule of one examination per year. The actual date of each visit was established by an independent administrative office. All patients had a diagnosis of CRD based on history, clinical findings, and ERG abnormalities. All patients gave informed consent to participate to the study, which adhered to the tenets of the Declaration of Helsinki and was approved by the Institutional Review Board.

TABLE. Patient Cohort

| Patient No.	Follow-up, y	Visits	Sex	Inheritance	Age, y	fERG, μV*	Baseline Values BCVA (Decimal)*	% of Normal Value	
								Rod ERG b-Wave*	Cone ERG b-Wave*
01	11.5	5	M	AR	48	0.30	1	80	60
02	6.2	8	M	AR	15	1.35	1	90	75
03	5.1	3	F	AR	30	0.6	0.05	60	45
04	6.2	4	M	AR	11	0.27	0.8	60	20
05	5	5	F	S	49	1.56	1	80	35
06	8.7	5	F	AR	59	0.34	0.9	70	65
07	3.2	5	F	AR	10	1.96	0.9	80	75
08	10	11	F	AR	20	0.65	0.45	70	35
09	4.1	5	M	S	13	0.79	0.5	60	25
10	5.4	5	F	AR	21	1.62	1	70	35
11	7.4	9	F	AR	11	0.35	0.2	75	25
12	4.7	5	F	AR	9	1.08	0.5	60	30
13	3.2	5	M	AR	28	0.26	0.6	80	45
14	7.4	9	F	AR	11	0.7	0.3	85	40
15	5.4	7	M	AR	10	1.75	0.2	80	30
16	3.8	6	F	AR	9	0.88	0.4	60	20
17	5.3	6	F	AR	41	0.73	0.3	80	20
18	8	9	F	AR	27	0.63	0.1	60	35
19	7.2	11	F	AR	42	0.33	0.2	60	25
20	8.6	6	M	AR	19	1.21	0.6	80	40
21	4	4	M	AR	13	0.32	0.3	90	30
22	9.8	14	M	S	11	0.13	0.9	90	50
23	2.7	4	M	AR	44	1.04	0.2	85	45
24	2.9	3	M	AR	11	1.65	0.65	85	25
25	12.6	20	F	AR	9	0.67	0.2	65	10
26	10.2	13	F	AR	36	0.52	0.3	50	10
27	5.9	5	F	AR	13	1.48	0.1	40	15
28	11.8	7	M	AR	25	0.29	0.4	80	8
29	9.4	3	F	AD	58	0.24	0.3	85	15
30	2.7	3	M	AR	36	0.64	0.05	50	25
31	3.4	5	F	AR	24	1.2	1	80	45
32	3	5	M	AR	10	1.27	0.9	80	55
33	10.2	9	F	S	27	1.22	0.4	95	25
34	5.8	6	M	AR	18	0.26	0.3	65	15
35	2.6	2	F	AR	20	1.61	0.5	75	30
36	10.4	2	M	AR	45	0.67	1	80	60
37	2.4	2	M	AR	39	2.125	1	80	40
38	2.9	2	M	AR	46	1.88	0.2	85	55
39	3	3	M	AR	12	1.2	1	85	25
40	3	3	F	AR	40	0.68	1	75	15
41	6.6	2	F	AR	22	2.54	0.2	65	25
42	11.3	2	F	AD	46	0.15	0.1	60	15
43	2.8	2	F	AR	36	0.44	0.2	85	35
44	4.6	2	F	AR	33	0.81	0.1	60	20
45	11.6	2	M	AR	49	2.2	0.3	65	15
46	2.6	2	M	AR	57	1.13	0.3	85	25
47	2.5	6	F	AR	11	1.36	0.8	65	15

AD, autosomal dominant; S, sporadic; AR, autosomal recessive.
* Average between the two eyes.

Inclusion Criteria

The long-term changes of fERG in CRD were evaluated in a cohort of 47 patients with a follow-up ≥2.5 years (Table) who met the following inclusion criteria: (1) typical CRD with a cone–rod pattern of retinal dysfunction (Fig. 1), as determined by International Society for Clinical Electrophysiology of Vision (ISCEV) standard Ganzfeld ERG,[16] dark-adapted Tuebinger perimetry, and classic fundus appearance; (2) inheritance pattern unequivocally determined by a detailed family and medical history; (3) no or minimal ocular media opacities; (4) absence of nystagmus; (5) foveal fixation or preferred retinal locus for fixation within 3° of the fovea and stable throughout the follow-up; (6) no concomitant ocular, visual, or systemic diseases; and (7) baseline age ≥9 years, as tests of younger children proved unreliable. The data set analyzed derived from 262 recording sessions performed from 1999 to 2012 under the same test conditions.
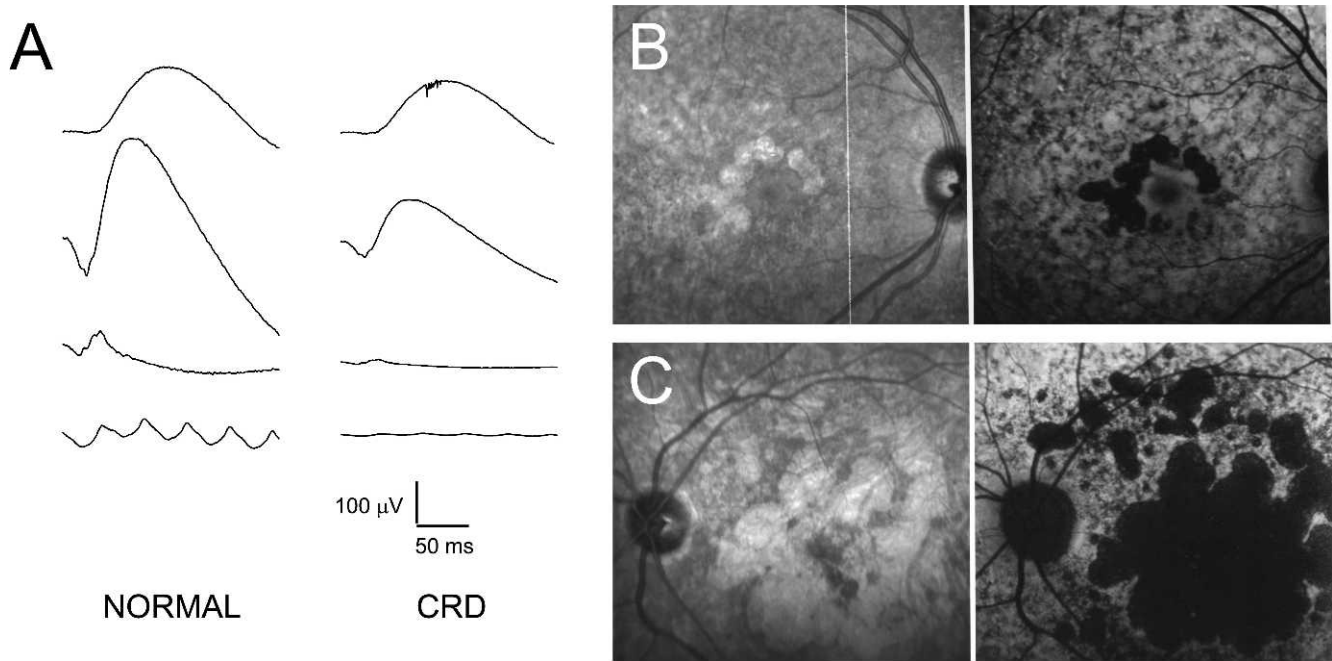
FIGURE 1. Representative Ganzfeld ERGs and fundus images of the CRD patients in the cohort. (**A**) Examples of ERG recordings according to ISCEV standard in a normal subject (*left*) and a representative CRD patient (patient No. 13 in the Table). *From top to bottom*: Rod response, mixed rod and cone response, single-flash cone response, 31-Hz flicker response. (Note that the patient's ERG shows a substantial loss of single-flash and flicker response, whereas rod and mixed responses are relatively spared, compared with the control ERG.) (**B**, **C**) Baseline fundus images from patient No. 31 (**B**), illustrating an early phase of the disease, and patient No. 30 (**C**), illustrating a late phase. *Left*: Infrared images. *Right*: Fundus autofluorescence.

Measures of Ocular Function and ERG

A full general and ophthalmologic examination (including detailed family history, anterior segment biomicroscopy, best corrected Snellen visual acuity, direct and indirect ophthalmoscopy, and IOP measurement) was performed on each patient at baseline and on several consecutive visits.

Macular focal cone ERG (fERG) was recorded from the central 18° region using a flickering uniform red field superimposed on a constant equiluminant steady adapting background minimizing stray-light modulation.[17,18] The stimulus was generated by a circular array of eight red light-emitting diodes (LEDs) (660 nm; 93 cd/m²) presented on the rear of a Ganzfeld bowl. A diffusing filter in front of the LED array made it appear as a circle of uniform red light. Macular focal cone ERGs were recorded in response to the 41-Hz sinusoidal 95% luminance modulation of the central red field. Patients fixated monocularly a 0.25° central fixation mark, under the constant
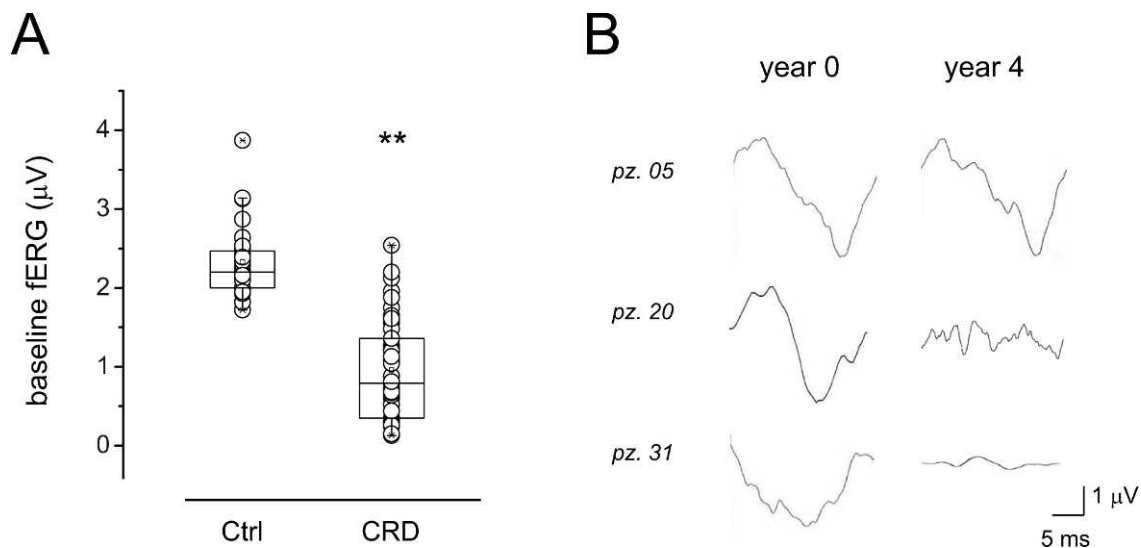
FIGURE 2. Reduced fERG amplitudes in CRD patients. (**A**) Baseline fERG values in normal control (Ctrl) and in the CRD patients of the study cohort. fERG values are average between the two eyes. Control values are from a cohort of 28 age-matched normal subjects recorded in the same conditions as the CRD patients. Average Ctrl fERG 2.33 ± 0.46 ($N = 28$), CRD baseline fERG 0.96 ± 0.61 ($N = 47$). The difference in fERG values is statistically significant ($P < 10^{-4}$ Mann-Whitney test). (**B**) Example of fERG recordings obtained at baseline and 4 years later from three CRD patients.
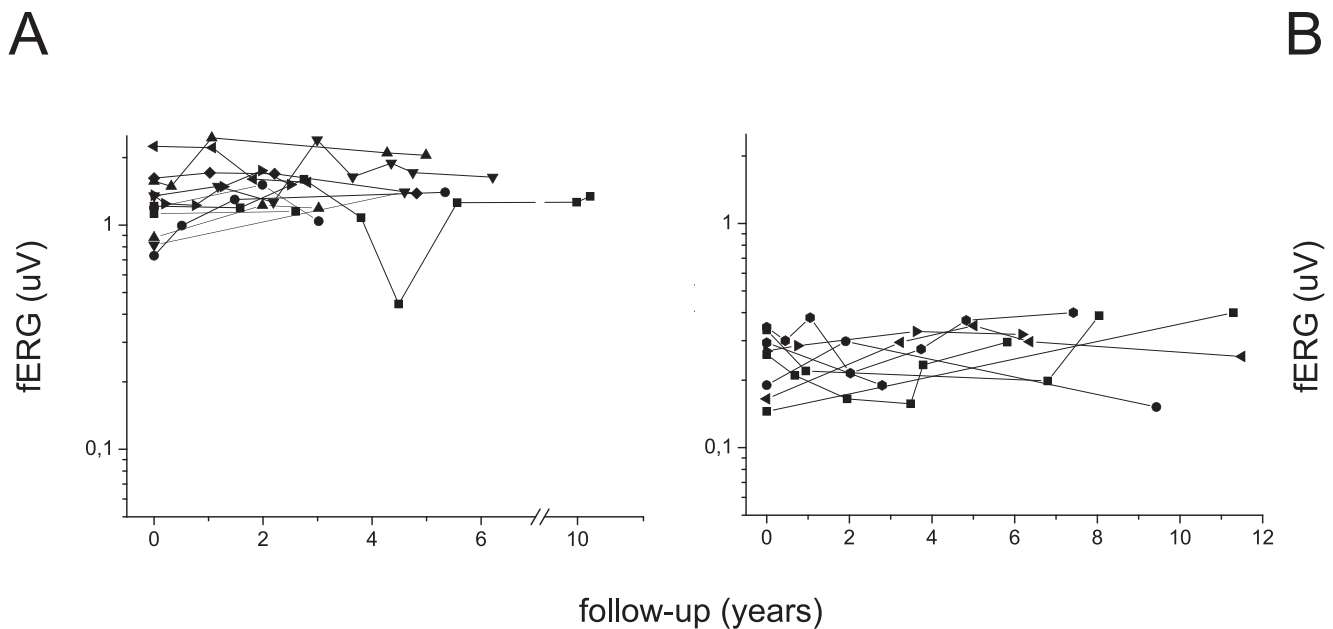
FIGURE 3. Macular focal cone ERG follow-up shows two distinct sets of stationary CRD patients. (**A**) fERG time courses of high-amplitude fERG stationary patients (fERG ≥1 µV). (**B**) Examples of fERG time courses for low-amplitude stationary patients (fERG ≤0.5 µV). In each panel, fERG is plotted on a logarithmic scale. Each *symbol* corresponds to a patient.

monitoring of an external observer. Pupils were pharmacologically (1% tropicamide and 2.5% phenylephrine hydrochloride) dilated to a diameter ≥8 mm, and all subjects underwent a 20-minute preadaptation period to the stimulus mean luminance. Macular focal cone ERG was recorded by means of an Ag-AgCl 0.9-cm diameter skin electrode taped on the skin of the lower eyelid, after coating the electrode surface with saline electroconductive gel. A similar electrode on the lower eyelid of the contralateral patched eye was used as reference.

For each recording, fERG signals were amplified (100,000-fold), bandpass filtered (1–100 Hz; 6 dB/octave), and averaged (12-bit resolution, 2-kHz sampling rate, 1200–1600 repetitions in 6–8 blocks). Off-line discrete Fourier analysis quantified the amplitude of the response first harmonic at 41 Hz. Two recordings (6–8 blocks each) were commonly acquired on each visit. In accordance with previous studies,[19] noise level was computed as the signal Fourier component at 45 Hz, a frequency different but very close (10% difference) to the real signal modulation frequency.

In this retrospective study, we could not rely on systematic recordings documenting short-term variability. Therefore, to determine a priori cutoff for repeatability of fERG recording in individual patients, we used within-session variability. This choice has the limitation of excluding some potential sources of variation such as pupil size or electrode placement. However, it has the advantage of being unaffected by the rapid decrease of fERG with time in fast-declining patients.

Data Analysis

Macular focal cone ERG decline over time was fitted with a simple exponential decay model in agreement with previous studies.[10,14] Since fERG amplitude distributions were skewed, individual fERG values were transformed into logarithms (base 10), followed by linear regression analysis of logfERG amplitude versus time. Linear regression analysis of individual patient fERG data showed no "ceiling" or "floor" effects (not shown), and thus no censoring was performed.[20,21] Between-group difference for fast- and slow-decaying patient sets was

evaluated by comparing the distributions of decay rates obtained by linear fitting of individual curves in either set. Average decay rate within either set was estimated by global linear fitting, a linear model that allows individual intercepts to vary with patients and optimizes the fit with a single decay-rate parameter (slope) common for all individual patient curves. The advantage of this model is the simultaneous use of the entire data set to determine a common average decay without external assumptions about weighting factors and modalities.[20,21]

Relationship Between Visual Acuity and fERG Changes

Best-corrected visual acuity (BCVA) values were expressed as log values of the minimum angle of resolution (MAR), in accordance with previous studies. Changes in BCVA with time were expressed as −ΔlogMAR (logMAR[time1] − logMAR [time2], with time2 subsequent to time1), to represent visual acuity losses with negative values. To study the relationship between fERG and VA variation, we considered every pair of visits where both fERG and VA were recorded in a patient, we computed −ΔlogMAR and Δlog fERG (log fERG[time2] − log fERG[time1]) for each eye, then we plotted together data obtained from all patients.

A Posteriori Receiver–Operator Characteristic (ROC) Curves for fERG Test Decay Detection and Bootstrap Analysis

This computation was performed in four steps. First, we obtained cumulative probability curves for fERG percentage loss between visits for each set of patients. Second, we computed specificity and sensitivity curves—where specificity is the likelihood of correct identification of stationary patients, and sensitivity is the likelihood of correct identification of decaying patients (whether fast or slow decaying). Third, we computed the corresponding ROC curves, which plot sensitivity as a function of (1-specificity). Fourth, we used bootstrap
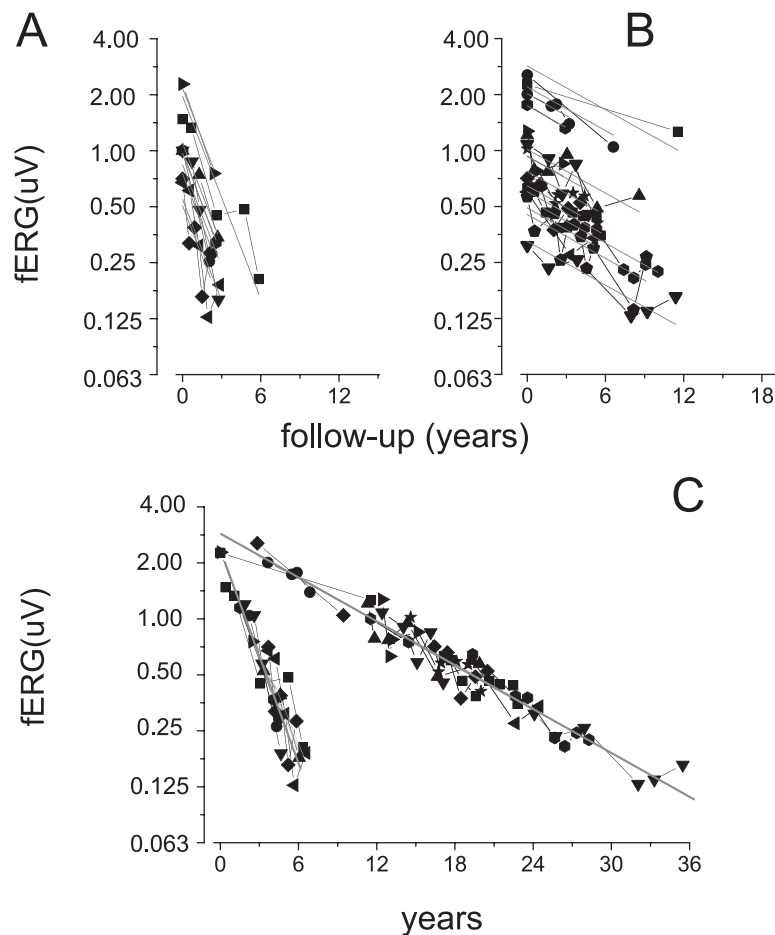
FIGURE 4. Two distinct clusters of fERG decay rates in progressive CRD forms. (**A**) Fast fERG decay was observed in nine patients, with an average loss of 34% fERG amplitude per year (95% CI, 28.4%–39.3%; global linear fit of logfERG data). Data are plotted on a logarithmic scale. Each *symbol* corresponds to a patient. *Gray lines* indicate the individual fit lines. (**B**) Slow fERG decay was observed in 13 patients, with an average loss of –8.6% fERG amplitude per year (95% CI, 7.1%–10.1%). Data are plotted on a logarithmic scale. Each *symbol* corresponds to a patient. *Gray lines* indicate the individual fit lines. (**C**) Fast- and slow-decaying fERG curves are replotted by shifting them along the abscissa in order to align each curve in either set along one fit line. The curve envelopes thus obtained illustrate the difference between the two decay behaviors over the years. Notice that none of the curves is normalized.

analysis to obtain the distribution of values for the area under the ROC curve, a standard means to evaluate the accuracy of a test. Specifically, for each patient and interval of time, we selected all the pairs of measures that were separated in time by the set interval. Chosen time intervals were 1, 2, and 3 years, each with 0.5-year tolerance (e.g., measures separated from 0.5 to 1.5 years were considered for the 1-year interval). For each pair of measures, we computed the difference between the more recent and the older measure and expressed it as the percentage of the latter. Pooling together measures from all patients in each category, we determined the corresponding cumulative probability curves. As expected, the cumulative probability curves for stationary patients did not significantly change with the time interval (not shown), and high and low stationary-patient curves coincided (not shown). From these probability curves, we computed sensitivity and specificity for discriminating decaying patients from stationary patients as a function of fERG threshold and built the corresponding ROC curves. For bootstrap analysis,[22] we focused on the data sets collecting fERG differences after 1 and 3 years. For each data set, we ran 10,000 bootstrap simulations. In bootstrap simulations, N data are extracted from the data set (where N is the total number of measures in the data set) allowing repetition, so that each measure can be extracted multiple times in each simulation

Statistical Analysis

Data were analyzed with Origin 8.5 (OriginLab Corporation, Northampton, MA) and GraphPad Prism 6.0 (GraphPad Software, Inc., La Jolla, CA). Unless otherwise specified, data are presented as mean ± standard deviation. Differences between two groups were compared using Student's *t*-test, or Mann-Whitney rank test in case of non-normal distributions. Differences in baseline ages across groups were compared using Kruskal-Wallis nonparametric test. Normality test was performed using the D'Agostino-Pearson omnibus K2 test. For linear regression, residuals were analyzed by the D'Agostino-Pearson omnibus K2 normality test, and run tests. Fit results were considered only when the fit converged and $P < 0.01$. Following established convention, the quality of fit was recorded as adjusted coefficient of determination (adjusted R^2 [Adj R^2]) and P value. Values obtained by best fitted regression lines are reported together with their 95% confidence interval (CI).

RESULTS

The study cohort consisted of 47 CRD patients (21 males and 27 females), with a total of 262 visits (Table). The average
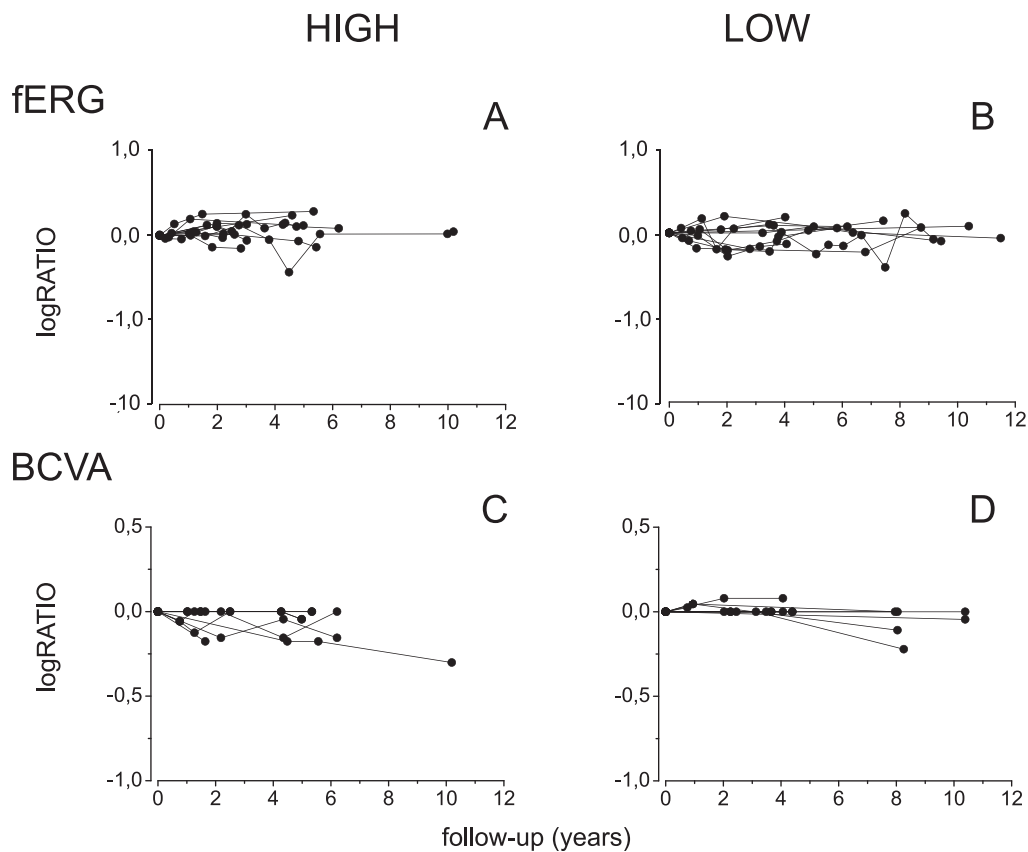
FIGURE 5. Macular focal cone ERG and BCVA follow-up in patients with stationary fERG. (**A**, **B**) fERG follow-up values plotted in log unit changes from baseline for patients with high (**A**) and low (**B**) stationary fERG. Time courses are for individual eyes. (**C**, **D**) BCVA follow-up values for individual eyes from patients with high (**C**) and low (**D**) stationary fERG. BCVA is plotted as log unit changes from baseline in the MAR.

follow-up was 6.1 ± 3.1 years (range, 2.5–12.6 years) with an average of 1.0 ± 0.5 visit per year. Age at baseline was 27.1 ± 15.7 years. Minimum age at baseline was 9 years, maximum age at final follow-up was 67 years. Unless otherwise specified, we averaged visual measures between the two eyes for the analysis.

fERG in CRD Patients

Most CRD patients in the cohort had baseline fERG responses smaller than those observed in normal individuals of similar age (Fig. 2A; control, $N = 28$; CRD, $N = 47$; $P < 0.05$ Mann-Whitney rank test). All CRD responses, however, remained well above noise level (average noise level at baseline, 0.03 ± 0.05 μV; $N = 47$). In the follow-up, fERG responses remained stationary for approximately half of the patients, while the remaining half experienced significant fERG reduction with time, as exemplified by the recordings from three patients in Figure 2B.

fERG Repeatability

To obtain preliminary cutoff criteria to discriminate stationary and progressive time courses, we analyzed fERG within-visit variability (see Methods section). For each patient, we compared the amplitude of the two fERG recordings obtained at baseline, expressing their difference as the percentage of their average, and used the fifth and 95th percentiles of the difference distribution across patients as cutoff limits for stationary fERG. Such limits were −56.9% and 52%, respectively. Therefore, we considered patients as declining when their fERG amplitude lost more than 56.9% of the baseline value

during follow-up, improving if the fERG amplitude increased by more than 52% of the baseline value, and stationary if their fERG changes remained within the cutoff limits. According to these criteria, 25 of the 47 cohort patients had a stationary fERG follow-up, while the remaining 22 patients showed an fERG declining with time. Follow-up duration did not significantly differ between stationary and decaying patients (Student's t-test; $P < 0.05$).

Stationary fERG Patients

In 25 of the 47 patients, fERG amplitude remained stationary during the follow-up. With rare occasional exceptions, 12 patients had fERG constantly ≥ 1 μV (Fig. 3A) and 13 had fERG ≤ 0.5 μV (Fig. 3B). Only 11 of the 131 measures obtained from stationary fERG patients fell within the 0.5- to 1-μV range. Baseline age was not significantly different between high (fERG >1 μV) and low (fERG <0.5 μV) stationary patients (high stationary, 29 ± 17 years; low stationary, 31 ± 19 years; $P = 0.6$ Mann-Whitney rank test).

Decaying fERG Patients

In 22 of the 47 patients, fERG amplitude declined with time. Macular focal cone ERG decline was either fast (Fig. 4A, nine patients) or slow (Fig. 4B, 13 patients). Global linear fitting gave an average annual fERG loss of 34.0% for fast-decaying patients (95% CI, 28.4%–39.3%; $N = 9$ patients, $df = 20$, Adj $R^2 = 0.79$), and 8.6% for slowly decaying patients (95% CI, 7.1%–10.1%; $N = 13$ patients, $df = 56$, Adj $R^2 = 0.91$). This 3-fold

FAST   SLOW
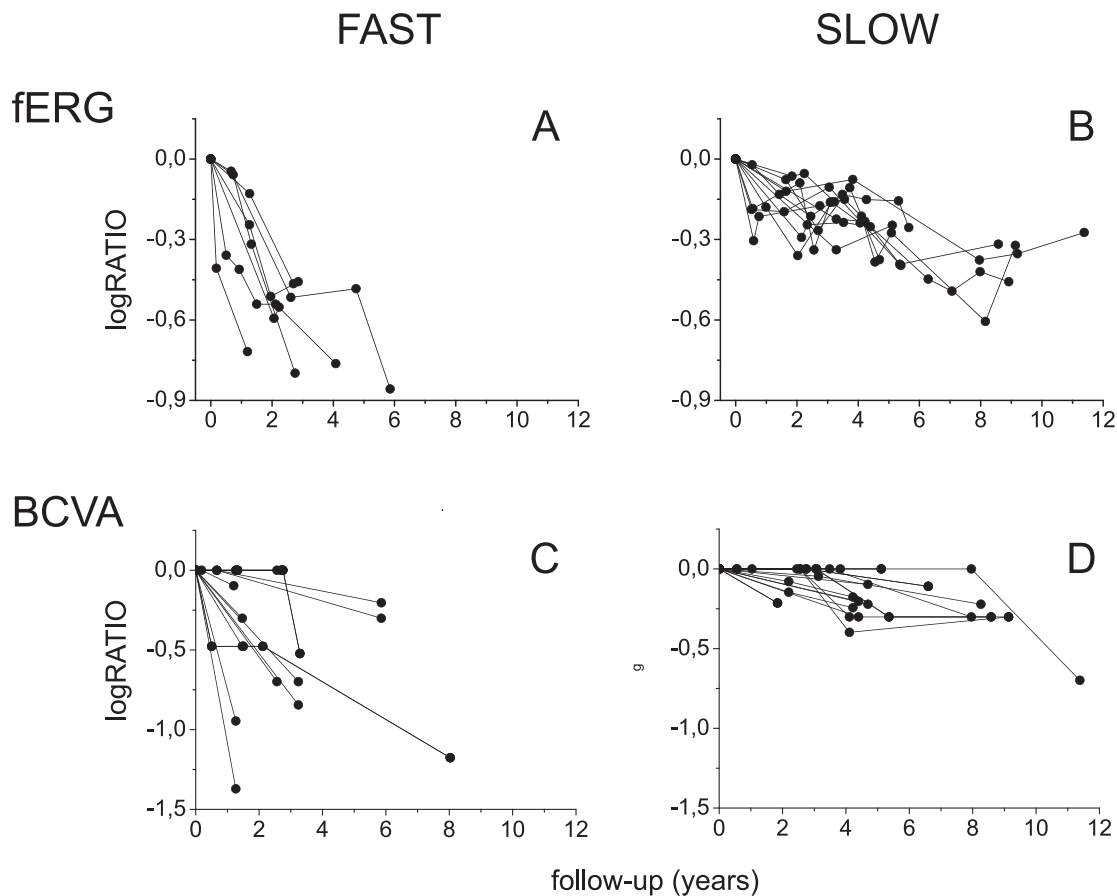
FIGURE 6. Macular focal cone ERG and BCVA follow-up in patients with decaying fERG. (A, B) fERG follow-up plotted in log unit changes from baseline for patients with fast (A) and slow (B) decaying fERG. Time courses are for individual eyes. (C, D) BCVA follow-up for individual eyes from patients with fast (C) and slow (D) decaying fERG. BCVA is plotted in log unit changes from baseline in the MAR.
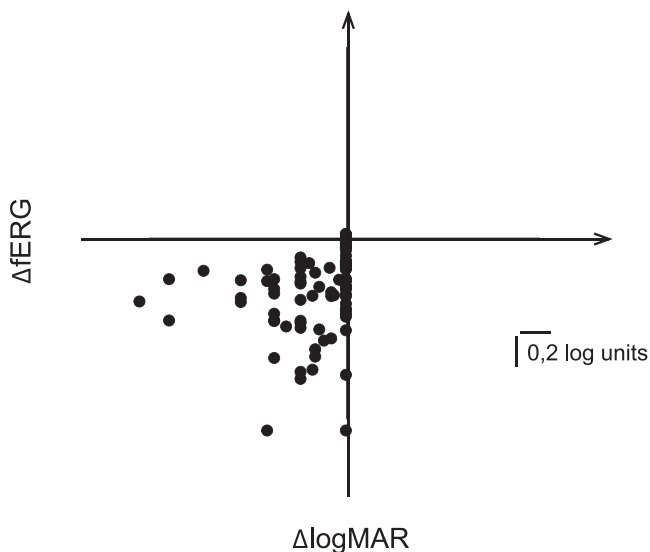
FIGURE 7. Macular focal cone ERG decline always accompanies and often anticipates BCVA decline. Intervisit variation in fERG as a function of BCVA variation from all patients with decaying fERG. BCVA is plotted as −logMAR. Both fERG and BCVA variations are plotted as log unit loss between the first and the second of the two visits, which are compared.

difference in decay rate was statistically significant (Mann-Whitney rank test, $P < 0.001$; see Methods section).

The fast- and slow-decaying curve sets spanned the same voltage range—from 1 to 2 μV to below 0.5 μV, suggesting that fast- and slow-decaying patients undergo the same functional decline, but with two quite different time courses. This finding is emphasized in Figure 4C, where the curves in each set are shifted along the abscissa to make their fit lines converge onto a single line, thus modeling the expected time span for overall decline in either set. Baseline age was not significantly different between fast- and slow-progressing patients (fast decaying, 25 ± 13 years; slow decaying, 22 ± 12 years; $P = 0.6$; Student's t-test), nor in general between any pair of patient groups identified by fERG follow-up (Kruskal-Wallis test; $P = 0.44$).

fERG and Visual Acuity Loss

To understand how the classification in stationary and decaying CRD patients according to fERG follow-up is related to the outcome of more established clinical tests, we compared the time courses of fERG and BCVA.

Long-term BCVA follow-up was available for 18 patients with stationary fERG and 19 patients with decaying fERG, and the two groups had very similar BCVA follow-up duration (5.1 ± 2.8 years for fERG-stationary patients and 5.5 ± 2.9 years for fERG-decaying patients, $P = 0.67$ Student's t-test). The fERG and BCVA time courses—expressed as relative changes from baseline—are illustrated in Figure 5 for patients with stationary
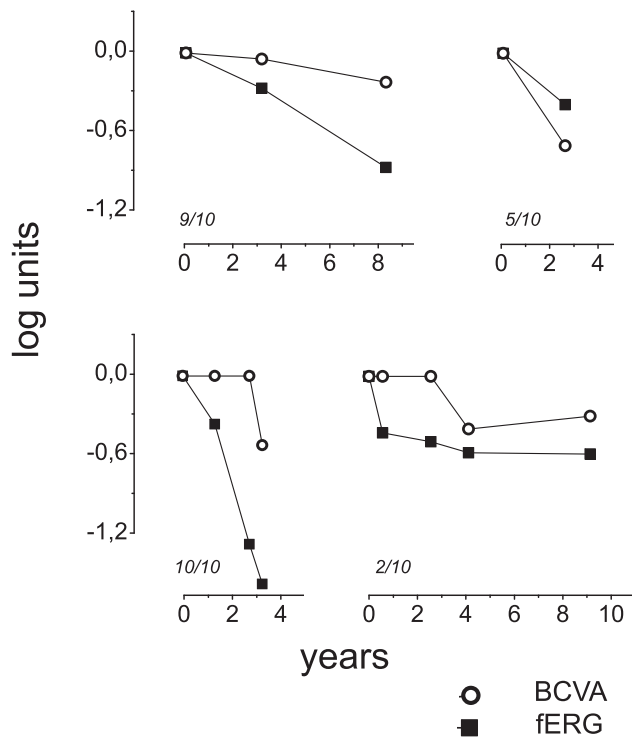
FIGURE 8. Examples of fERG and BCVA decline in individual CRD eyes. *Solid squares* are fERG data; *open circles* are BCVA data. *Top*: Concomitant onset of fERG and BCVA decline from baseline. *Bottom*: BCVA decline onset several years after fERG decline onset. Measures are normalized to baseline to show their relative decline. BCVA is quantified as MAR. fERG data are reported only when corresponding BCVA measures existed. For each case, baseline BCVA is indicated in decimal.

fERG and in Figure 6 for fERG-decaying patients. On the average, patients with stationary fERG (Fig. 5) experienced little if any BCVA loss with time, with an average maximum decay of −13% (−0.06 ± 0.07 log units; $N = 36$ eyes) in their minimum angle of resolution (MAR). On the contrary, patients with decaying fERG (Fig. 6) had an average loss in MAR with time of −55% (−0.35 ± 0.33 log units; $N = 38$ eyes), and all experienced BCVA decline with time (Fig. 6), excluding two patients whose baseline acuity was already below 0.1 decimals. Taken together, these data show that fERG follow-up discriminates stationary and progressive CRD forms in close agreement with the discrimination derived from BCVA follow-up.

We next analyzed how fERG losses related to BCVA losses in decaying patients. Considering individual eye measures, we found that all BCVA losses (55/55; $N = 38$ eyes; 19 patients) corresponded to a simultaneous fERG loss in the same eye (Fig. 7). However, fERG losses could occur without BCVA loss; in 65% of the cases (36/55) a BCVA loss was also preceded by a fERG loss, which was detected while the patient's acuity was still stable. These events are exemplified for individual cases in Figure 8.

These results were quantified in terms of BCVA survival probability following fERG loss in decaying patients (Fig. 9). Specifically, for all decaying patients, we computed the time between the first fERG loss from baseline and the first BCVA loss (upper curve), as well as the time between the first fERG loss and the last visit where the BCVA was still at baseline (lower curve), reasoning that the two curves represent an upper and a lower bound, respectively, for BCVA survival
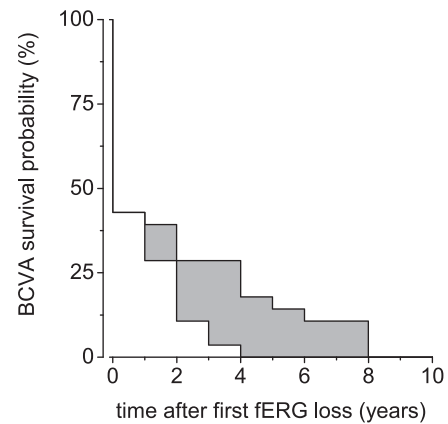
FIGURE 9. BCVA survival probability as a function of time after first fERG loss from baseline in progressive CRD patients. The *upper curve* is the time between first fERG loss from baseline and first BCVA loss, the *lower curve* is the maximum time BCVA stayed constant after first fERG drop. The two curves represent an upper and a lower bound, respectively, for BCVA survival probability. This analysis is based on $N = 32$ eyes, 17 patients. Patients with baseline BCVA <0.1 decimal were not included, as they were considered already at the minimum BCVA reliably detectable by Snellen.

probability. In all decaying patients, we found that when fERG declines, BCVA is doomed to do so, although in half of the patients, BCVA can survive several years after the first fERG loss (Fig. 9).

A Posteriori ROC Curves for fERG Decay Detection

The analysis hereto described began by setting a priori criteria to discriminate stationary and decaying fERG time-courses. A posteriori, more realistic cutoff criteria can be determined by knowing the behavior of stationary and decaying fERG time curves. Specifically, one can use the data set to compute the likelihood of a correct identification of a decaying patient (sensitivity), and the corresponding risk of mistaking a stationary patient for a progressing one (1-specificity), as a function of fERG decay cutoff. The resulting specificity and sensitivity curves as a function of fERG decay threshold at 1 and 3 years from baseline are shown in Figure 10A (continuous lines). The corresponding ROC curves for 1- and 3-year follow-up are shown in Figure 10B. The area under the ROC curve—commonly used as a measure of test accuracy[23]—is 0.74 at 1 year (0.69–0.79, fifth to 95th percentiles) and 0.825 at 3 years (0.77–0.87, fifth to 95th percentiles). The fifth to 95th percentile intervals indicated are obtained by running 10,000 bootstrap simulations for each data set (1 and 3 years), computing the area under the ROC curve for each simulation and the overall distribution of the latter from all the simulations of each data set (Fig. 10C).

DISCUSSION

This retrospective study shows that fERG follow-up leads to a clear-cut subdivision of CRD patients in stationary or decaying, providing quantitative criteria defining each typology. Stationary patients had fERG amplitudes that remained either above 1 μV or below 0.5 μV, with a few occasional exceptions. Decaying patients had either a slow (7%–10% annual loss) or a fast (28%–39% annual loss) decaying fERG, spanning in time from above 1 μV to below 0.5 μV. Baseline age did not significantly differ between high-stationary, fast-, and slow-decaying patients, suggesting that these different fERG time
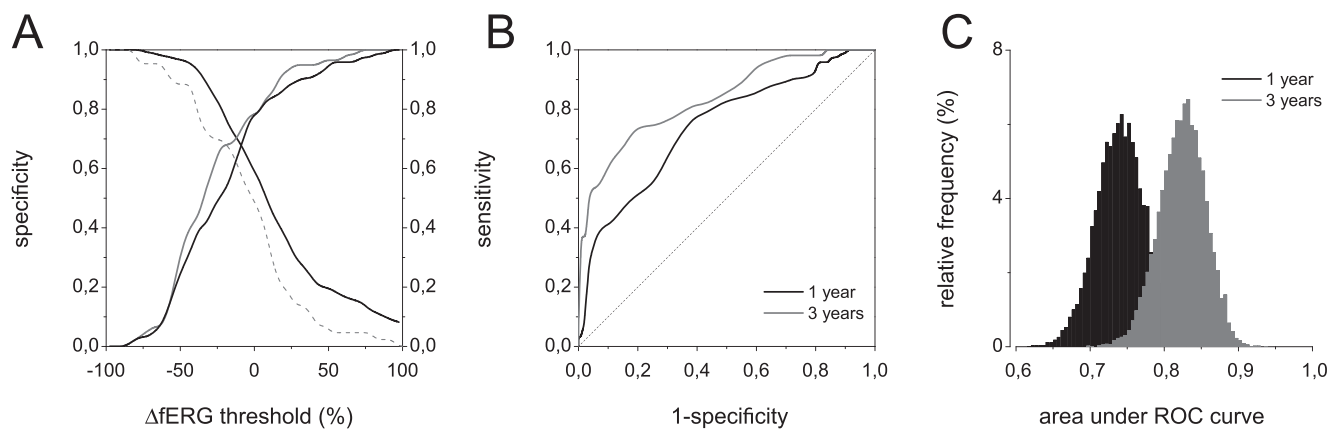
FIGURE 10. Receiver-operator characteristic (ROC) curves for fERG decay detection test. (**A**) Specificity and sensitivity as a function of the minimum fERG loss chosen to indicate a true decay (cutoff threshold) at 1 and 3 years from baseline, as derived from a posteriori data set analysis (1 year, *continuous black line*; 3 years, *continuous gray line*). *Dashed line* is the specificity derived a priori from intervisit variability. (**B**) ROC curves for fERG decay test at 1 and 3 years from baseline. (**C**) Mean and distribution of the area under the ROC curves obtained from bootstrap analysis at 1 year (*black*) and 3 years (*gray*) from baseline.

courses reflect different phenotypes and not just different stages of the disease.

The subdivision of CRD forms into stationary and progressive is consistent with the standard categorization based on subjective symptoms and clinical signs recorded with a variety of techniques.[1,2,4] The existence of fast- and slow-progressing CRD forms has been reported in previous studies, although few diagnostic measures until now provided a clear-cut separation of the two. Microperimetric studies document fast and slow progression rates for the increase of cone relative threshold over time,[12] and for the sensitivity at the lesion border[24] in CRD patients. Similarly, fast and slow progression rates have been reported for the enlargement of the central scotoma in CRD.[25] Of interest, the range of decay rates found with fERG follow-up overlaps with the range of decay rates identified in previous studies.[12,14,24,25] This finding suggests that, with different degrees of sensitivity and reliability, fERG parallels other techniques in detecting the progression of common biological processes underlying central retinal dysfunction in CRD.

fERG and Visual Acuity Progression

Best-corrected visual acuity is a measure of central retina functionality of enormous impact on a patient's daily life. For this reason, we analyzed how fERG follow-up compared with BCVA time course in terms of reliability, effectiveness, and early detection of individual risk of visual decay in CRD patients.

We found that fERG discriminates stationary and progressive CRD forms in agreement with BCVA follow-up: patients with stationary fERG experienced very limited acuity loss with time, while patients with decaying fERG experienced significant BCVA decline with time. Moreover, we found that BCVA losses in decaying patients were always accompanied by fERG amplitude losses. The reverse was not true, as fERG losses could anticipate BCVA losses. Indeed, BCVA could survive several years after the first fERG loss, although it eventually decayed.

Taken together, these results demonstrate that fERG follow-up offers high diagnostic reliability and a precocious sensitivity to disease progression that always detects acuity losses and can often anticipate them for several years.

Accuracy of fERG Follow-up for Early Decay Detection

The fERG repeatability cutoff range defined a priori on the basis of intravisit variability was comparable with that reported for psychophysical techniques in CRD with known genotype.[10,26] However, the stereotyped behavior of fERG curves allowed an a posteriori analysis of the data set to obtain more realistic cutoff criteria and determine the accuracy of the test. This analysis showed that threshold for fERG decay detection can be lowered considerably with respect to the initial conservative cutoff. This same analysis, combined with bootstrap, produced ROC curves that can be used to estimate the accuracy of fERG follow-up in determining whether patients are stationary or decaying. The resulting areas under the ROC curve—0.74 at 1 year and 0.825 at 3 years—place the test in the high-accuracy ranks according to standard classification.[23]

CONCLUSIONS: PRO AND CONTRA OF fERG

To our knowledge, no other study has employed the long-term follow-up of central retina ERG recordings to longitudinally evaluate the functional decline in CRD patients. Here, we showed that fERG represents a direct and sensitive assay to detect, categorize, and follow the progression of central retinal dysfunction in CRD. This approach may help anticipate, for an individual patient, the likelihood and rate of further disease progression before visual acuity loss has occurred.

Macular focal cone ERG follow-up cannot replace any of the presently available diagnostic techniques for CRD: it lacks the fine spatial details detectable with multifocal ERG[27] and microperimetry,[10] has no clear relation to real life as visual acuity does, nor the diagnostic sensitivity of eye imaging.[15] Yet, its reliable, clear-cut, and precocious determination of individual patient risk of decay strongly commends its inclusion among the primary diagnostic tools for CRD.

References

1. Hamel CP. Cone rod dystrophies. *Orphanet J Rare Dis*. 2007;2: 7.

2. Michaelides M, Hardcastle AJ, Hunt DM, Moore AT. Progressive cone and cone-rod dystrophies: phenotypes and underlying molecular genetic basis. *Surv Ophthalmol*. 2006;51:232–258.

3. Berson EL, Gouras P, Gunkel RD. Progressive cone-rod degeneration. *Arch Ophthalmol*. 1968;80:68–76.

4. Heckenlively JR. RP cone-rod degeneration. *Trans Am Ophthalmol Soc*. 1987;85:438–470.

5. Thiadens AA, Phan TM, Zekveld-Vroon RC, et al. Clinical course, genetic etiology, and visual outcome in cone and cone-rod dystrophy. *Ophthalmology*. 2012;119:819–826.

6. Yagasaki K, Jacobson SG. Cone-rod dystrophy: phenotypic diversity by retinal function testing. *Arch Ophthalmol*. 1989; 107:701–708.

7. Yagasaki K, Jacobson SG, Apathy PP, Knighton RW. Rod and cone psychophysics and electroretinography: methods for comparison in retinal degenerations. *Doc Ophthalmol*. 1988; 69:119–130.

8. Ripps H, Noble KG, Greenstein VC, Siegel IM, Carr RE. Progressive cone dystrophy. *Ophthalmology*. 1987;94:1401–1409.

9. Lois N, Holder GE, Bunce C, Fitzke FW, Bird AC. Phenotypic subtypes of Stargardt macular dystrophy-fundus flavimaculatus. *Arch Ophthalmol*. 2001;119:359–369.

10. Cideciyan AV, Swider M, Aleman TS, et al. Macular function in macular degenerations: repeatability of microperimetry as a potential outcome measure for ABCA4-associated retinopathy trials. *Invest Ophthalmol Vis Sci*. 2012;53:841–852.

11. Thiadens AA, Soerjoesing GG, Florijn RJ, et al. Clinical course of cone dystrophy caused by mutations in the RPGR gene. *Graefes Arch Clin Exp Ophthalmol*. 2011;249:1527–1535.

12. Cideciyan AV, Swider M, Aleman TS, et al. ABCA4 disease progression and a proposed strategy for gene therapy. *Hum Mol Genet*. 2009;18:931–941.

13. Fujinami K, Lois N, Davidson AE, et al. A longitudinal study of Stargardt disease: clinical and electrophysiologic assessment, progression, and genotype correlations. *Am J Ophthalmol*. 2013;155:1075–1088; e13. doi:10.1016/j.ajo.2013.01.018

14. Birch DG, Anderson JL, Fish GE. Yearly rates of rod and cone functional loss in retinitis pigmentosa and cone-rod dystrophy. *Ophthalmology*. 1999;106:258–268.

15. Fishman GA, Jacobson SG, Alexander KR, et al. Outcome measures and their application in clinical trials for retinal degenerative diseases: outline, review, and perspective. *Retina*. 2005;25:772–777.

16. Marmor M, Arden G, Nilsson S, Zrenner E. Standard for clinical electroretinography. International Standardization Committee. *Arch Ophthalmol*. 1989;107:816–819.

17. Iarossi G, Falsini B, Piccardi M. Regional cone dysfunction in retinitis pigmentosa evaluated by flicker ERGs: relationship with perimetric sensitivity losses. *Invest Ophthalmol Vis Sci*. 2003;44:866–874.

18. Falsini B, Iarossi G, Fadda A, et al. The fundamental and second harmonic of the photopic flicker electroretinogram: temporal frequency-dependent abnormalities in retinitis pigmentosa. *Clin Neurophysiol*. 1999;110:1554–1562.

19. Porciatti V, Burr DC, Morrone MC, Fiorentini A. The effects of aging on the pattern electroretinogram and visual evoked potential in humans. *Vision Res*. 1992;32:1199–1209.

20. Berson EL, Rosner B, Weigel-DiFranco C, Dryja TP, Sandberg MA. Disease progression in patients with dominant retinitis pigmentosa and rhodopsin mutations. *Invest Ophthalmol Vis Sci*. 2002;43:3027–3036.

21. Falsini B, Galli-Resta L, Fadda A, et al. Long-term decline of central cone function in retinitis pigmentosa evaluated by focal electroretinogram. *Invest Ophthalmol Vis Sci*. 2012;53: 7701–7709.

22. Efron B, Tibshirani RJ. *An Introduction to the Bootstrap (Monographs on Statistics and Applied Probability)*. Vol. 57. New York: Chapman & Hall; 1993.

23. Simundic A-M. Measures of diagnostic accuracy: basic definitions. *eJIFCC*. 2008;19. Available at: www.ifcc.org/ifccfiles/docs/190404200805.pdf. Accessed September 24, 2013.

24. Chen FK, Patel PJ, Webster AR, et al. Nidek MP1 is able to detect subtle decline in function in inherited and age-related atrophic macular disease with stable visual acuity. *Retina*. 2011;31:371–379.

25. Zahid S, Jayasundera T, Rhoades W, et al. Clinical phenotypes and prognostic full-field electroretinographic findings in Stargardt disease. *Am J Ophthalmol*. 2012;155:465–473.

26. Roman AJ, Cideciyan AV, Schwartz SB, et al. Intervisit variability of visual parameters in Leber congenital amaurosis caused by RPE65 mutations. *Invest Ophthalmol Vis Sci*. 2013; 54:1378–1383.

27. Kretschmann U, Gendo K, Seeliger M, Zrenner E. Multifocal ERG recording by the VERIS technique and its clinical applications. *Dev Ophthalmol*. 1997;29:8–14.